

SDR: Efficient Neural Re-ranking using Succinct Document Representation

Nachshon Cohen*, Amit Portnoy*, Besnik Fetahu, and Amir Ingber

ABSTRACT

BERT based ranking models have achieved superior performance on various information retrieval tasks. However, the large number of parameters and complex self-attention operation come at a significant latency overhead. To remedy this, recent works propose late-interaction architectures, which allow pre-computation of intermediate document representations, thus reducing the runtime latency. Nonetheless, having solved the immediate latency issue, these methods now introduce storage costs and network fetching latency, which limits their adoption in real-life production systems.

In this work, we propose the Succinct Document Representation (SDR) scheme that computes *highly compressed* intermediate document representations, mitigating the storage/network issue. Our approach first reduces the dimension of token representations by encoding them using a novel autoencoder architecture that uses the document’s textual content in both the encoding and decoding phases. After this token encoding step, we further reduce the size of entire document representations using a modern quantization technique.

Extensive evaluations on passage re-ranking on the MSMARCO dataset show that compared to existing approaches using compressed document representations, our method is highly efficient, achieving 4x–11.6x better compression rates for the same ranking quality.

1 INTRODUCTION

Information retrieval (IR) systems traditionally comprise of two stages: retrieval and ranking. Given a user query, the role of the retrieval stage is to quickly retrieve a set of candidate documents from a (very large) search index. The retrieval algorithm is typically fast but not accurate enough; in order to improve the quality of the end result for the user, the candidate documents are re-ranked using a more accurate but computationally expensive algorithm.

Large deep learning models have achieved the state of the art ranking performance in IR applications [44]. Transformer networks such as BERT [9] consistently show better ranking effectiveness at the cost of a higher computational cost and latency [34].

To rank k documents, the ranker is called k times with an input of the form (query, document), where the query is the same, but the document is different. Several works [4, 5, 13, 13, 26, 29, 33] have proposed to modify BERT-based rankers in a way that allows part of the model to compute query and document representations separately, and then produce the final score using a low-complexity interaction block (we denote these models as late-interaction rankers, see Fig. 2). With this approach, the document representations can be pre-computed in order to improve latency significantly: during runtime, the model computes the query representation (once), retrieves the pre-computed document representations, and only runs the interaction block k times to produce the final ranking score.

Precomputing document representations have been shown to significantly reduce latency while at the same time retaining comparable

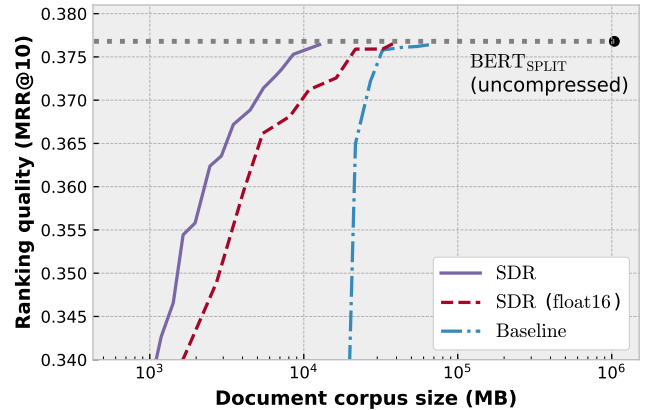


Figure 1: High-level contribution: MRR@10 performance vs. document corpus size tradeoff, measured on the MSMARCO-DEV dataset. BERT_{SPLIT} is a distilled late-interaction model with reduced vector width and no compression (§ 4.3). For MRR@10 above 0.35, SDR is 4x–11.6x more efficient compared to the baseline.

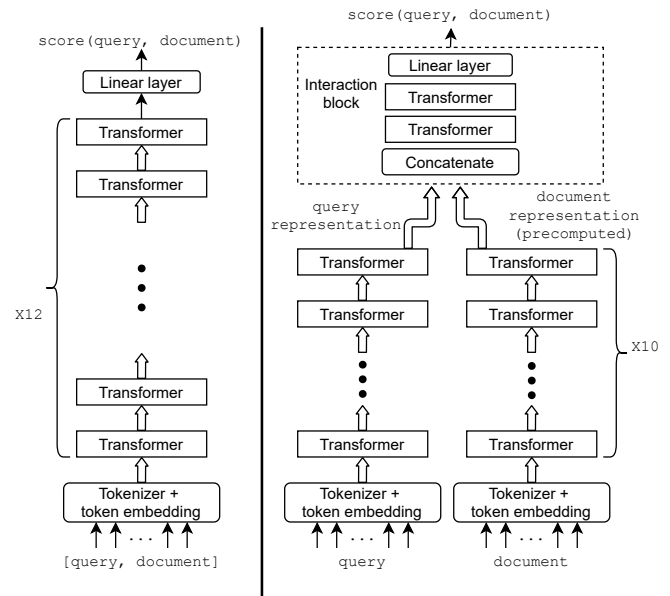


Figure 2: Left: BERT ranker. Right: late-interaction ranker (with two transformer layers as the interaction block).

*Both authors contributed equally to the paper.

scores to BERT models [13]. However, this does not account for additional storage and/or network fetching latency costs: these representations typically consist of the contextual token embeddings in a transformer model, which translate to orders of magnitude larger space requirements than storing the entire corpus search index¹.

In this work, we propose Succinct Document Representation (SDR), a general scheme for compressing document representations. Our scheme enables late-interaction rankers to be efficient in both latency and storage while maintaining high ranking quality. SDR is suitable for any ranking scheme that relies on contextual embeddings and achieves extreme compression ratios (2-3 orders of magnitude) with little to no impact on retrieval accuracy. SDR consists of two major components: (1) embedding dimension reduction using an *autoencoder* with *side information* and (2) *distribution-optimized quantization* of the reduced-dimension vectors.

In SDR, the autoencoder consists of two subnetworks: an encoder that reduces the vector’s dimensions and a decoder that reconstructs the compressed vector. The encoder’s output dimension represents the tradeoff between reconstruction fidelity and storage requirements. To improve the compression-reliability tradeoff, we leverage *static* token embeddings, which are available given that the ranker has access to the document text (as it needs to render it to the user), and are computationally cheap to obtain. We feed these embeddings to both the encoder and decoder as *side information*, allowing the autoencoder to focus more on storing “*just the context*” of a token, and less on its original meaning that is available in the *static* embeddings. Ablation tests verify that adding the static vectors significantly improves the compression rates for the same ranker accuracy.

Since data storage is measured in bits rather than floating-point numbers, SDR uses quantization techniques to reduce storage size further. Given that it is hard to evaluate the amount of information in each of the encoder’s output dimensions, we perform a randomized Hadamard transform on the vectors, resulting in (1) evenly spread information across all coordinates and (2) transformed vectors that follow a Gaussian-like distribution. We utilize known quantization techniques to represent these vectors using a small number of bits, controlling for the amount of quantization distortion.

Existing late-interaction schemes either ignore the storage overhead, or consider basic compression techniques, such as a simple (1 layer) autoencoder and float16 quantization. However, this is insufficient to reach reasonable storage size [29]; furthermore, fetching latency is unacceptable for interactive systems (cf. Appendix A). As an underlying late-interaction model we use a distilled model with a reduced vector width [20]. As a baseline compression scheme, we use a non-linear autoencoder consisting of 2 dense layers followed by float16 quantization, a natural extension of [29]. On the MSMARCO dataset, this baseline achieves compression rates of 30x with no noticeable reduction in retrieval accuracy (measured with the official MRR@10 metric). On top of this strong baseline, our SDR scheme achieves an additional compression rate of between 4x to 11.6x with the same ranking quality, reducing document representation size to the same order of magnitude as the retrieved text itself. In Figure 1 we include a high-level presentation of the baseline, a variant of our method with float16 quantization, and our full method.

¹In Appendix A, we also demonstrate how the latency introduced by such an increase in storage requirements can dominate the end-to-end latency.

To summarize, here are the contribution of this work:

- We propose the Succinct Document Representation (SDR) scheme for compressing the document representations required for fast Transformer-based rankers. The scheme is based on a specialized autoencoder architecture and subsequent quantization.
- For the MSMARCO passage retrieval task, SDR shows compression ratios of 121x with no noticeable decrease in ranking performance. Compared to existing approaches for producing compressed representations, our method attains better compression rates (between 4x and 11.6x) for the same ranking quality.
- We provide a thorough analysis of the SDR system, showing that the contribution of each of the components to the compression-ranking effectiveness is significant.

2 RELATED WORK

Late-interaction models. The idea of running several transformer layers for the document and the query independently, and then combining them in the last transformer layers, was developed concurrently by multiple teams: PreTTR [29], EARL [12], DC-BERT [33], DiPair [5], and the Deformer [4]. These works show that only a few layers where the query and document interact are sufficient to achieve results close to the performance of a full BERT ranker at a fraction of the runtime cost. For each document, the contextual token vectors are stored in a cache and retrieved during the document ranking phase. This impacts both storage cost (storing token contextual vectors for all documents) as well as latency cost of fetching these vectors during the ranking phase. MORES [13] is an extension of the late-interaction models, where in the last interaction layers, the query attends to the document, but not vice versa, and without document self-attention. As the document is typically much longer, this modification results in an additional performance improvement with similar storage requirements. ColBERT [26] is another variant that runs all transformer layers independently for the query and the document, and the interaction between the final vectors is done through a sum-of-max operator. In a similar line of work, the Transformer-Kernel (TK) [21], has an interaction block based on a low-complexity kernel operation. Both ColBERT and TK result in models with lower runtime latency at the expense of a drop in ranking quality. However, the storage requirements for both approaches are still significant.

Some of the works above acknowledge the issue of storing the pre-computed document representations and proposed partial solutions. In ColBERT [26], the authors proposed to reduce the dimension of the final token embedding using a linear layer. However, even moderate compression ratios caused a drop in ranking quality. In the PreTTR model [29], it was proposed to address the storage cost by using a standard auto-encoder architecture and the float16 format instead of float32. Again, the ranking quality drops even with moderate compression ratios (they measured up to 12x).

Several other works [18, 25, 28, 35, 43] proposed representing the queries and documents as vectors (as opposed to a vector per token), and using a simple function (e.g., the dot product or cosine distance) as the interaction block. While this ranker architecture approach is simple (and can also be used for the retrieval step via an approximate nearest neighbor search such as FAISS [24] or ScaNN

[16]), the overall ranking quality is generally lower compared to methods that employ a query-document cross-attention interaction.

Knowledge distillation. Knowledge distillation techniques, such as DistilBERT [38] and TinyBERT [23], can reduce the size of a model at a small cost in terms of quality. Such works were successfully applied for ranking [6, 20] and do not require storing document vectors. However, distillation works best when the distilled model has at least 6 layers. With just 2-3 layers, late interaction models generally achieve better quality than distillation models by smartly using the precomputed document representations.

Compressed embeddings. Our work reduces storage requirements by reducing the number of bits per floating-point value. Quantization gained attention and success in reducing the size of neural network parameters [10, 17, 41, 42] and distributed learning communication costs [2, 27, 39, 40]. Specifically, compressing word embeddings has been studied as an independent goal. May et al. [30] studied the effect of quantized word embeddings on downstream applications and proposed a metric for quantifying this effect with simple linear models that operate on the word embeddings directly. As our work is concerned with compressing *contextual* embeddings, these methods do not apply since the set of possible embeddings values is not bounded by the vocabulary size. Nevertheless, as in [30], we also observe that simple quantization schemes are quite effective. Our work uses recent advances in this area to further reduce storage requirements for document representation, which, to the best of our knowledge, were not previously attempted in this context.

3 SUCCINCT DOCUMENT REPRESENTATION (SDR)

Our work is based on the late-interaction architecture [4, 5, 13, 29, 33], which separates BERT into L independent layers for the documents and the queries, and $T - L$ interleaving layers, where T is the total number of layers in the original model, e.g., 12 for BERT-Base. Naively storing all documents embeddings consumes a huge amount of storage with a total of $m \cdot h \cdot 4$ bytes per document, where m is the average number of tokens per document and h is the model hidden size (384 for the distilled version we use). For MSMARCO, with 8.8M documents and $m=76.9$, it leads to a high storage cost of over a terabyte, which is not affordable except in large production systems.

Our compression scheme for the document representations consists of two sequential steps, (i) dimensionality reduction and (ii) block-wise quantization, described in § 3.1 and § 3.2 respectively.

3.1 Dimensionality Reduction using an AutoEncoder with Side Information (AESI)

To compress document representations, we reduce the dimensionality of token representations (i.e., the output of BERT’s L -th layer) using an autoencoder. Standard autoencoder architectures typically consist of a neural network split into an encoder and a decoder: the encoder projects the input vector into a lower-dimension vector, which is then reconstructed back using the decoder.

Our architecture, AESI, extends the standard autoencoder by using the document’s text as *side information* to both the encoder and decoder. Such an approach is possible since, no matter how the document scores are computed, re-ranking systems have access to

the document’s text in order to render it back to the user. In the rest of this section, we add the precise details of the AESI architecture.

Side Information. In line with our observation that we have access to the document’s raw text, we propose utilizing the *token embedding* information, which is computed by the embedding layer used in BERT’s architecture. The token embeddings encode rich semantic information about the token itself; however, they do not fully capture the context in which they occur; hence, we refer to them as *static embeddings*. For example, through token embeddings, we cannot disambiguate between the different meanings of the token *bank*, which can refer to either a geographical location (e.g., “river bank”) or a financial institution, depending on the context.

Static embeddings are key for upper BERT layers, which learn the contextual representation of tokens via the self-attention mechanism. We use the static embeddings as side information to both the encoder and decoder parts of the autoencoder. This allows the model to focus on encoding the *distilled context*, and less on the token information since it is already provided to the decoder directly. Encoding only the context is an easier task, allowing AESI to achieve higher compression rates, and at the same time, retaining the quality of the contextual representation.

AESI Approach. For a token whose representation we wish to compress, our approach proceeds as follows. We take the L -th layer’s output contextual representation of the token together with its static embedding and feed both inputs to the autoencoder. The information to be compressed (and reconstructed) is the contextual embedding, and the side-information, which aids in the compression task, is the static embedding. The decoder takes the encoder output, along with the static embedding, and attempts to reconstruct the contextual embedding. Figure 3 shows the AESI architecture.

With the AESI approach, there are several parameters that we determine empirically. First, the L -th transformer layer of the contextual representation that is provided as input, which has a direct impact on latency². Second, the size of the encoder’s output directly impacts the compression rate and thus storage costs.

Encoding starts by concatenating the input vector (i.e., the output of layer L , the vector we compress) and the static token embedding (i.e., the output of BERT’s embedding layer), and then passes the concatenated vector through an encoder network, which outputs a c -dimensional *encoded vector*. Decoding starts by concatenating the encoded vector with the static token embedding, then passes the concatenated vector through a decoder layer, which reconstructs the input vector. Specifically, we use a two-layer dense network for both the encoder and the decoder, which can be written using the following formula:

$$e = E(v, u) := W_2^e \cdot (\text{gelu}(W_1^e(v; u))) \quad (1)$$

$$v' = D(e, u) := W_2^d \cdot (\text{gelu}(W_1^d(e; u))) \quad (2)$$

where $v \in \mathbb{R}^h$ is the contextualized token embedding (the output of the L -th layer), $u \in \mathbb{R}^h$ is the static token embedding (the output of the embedding layer, which is the input to BERT’s layer 0 and includes token position embeddings and type embeddings), and $u; v$ means concatenation of these vectors. $W_1^e \in \mathbb{R}^{i \times 2h}$, $W_2^e \in \mathbb{R}^{c \times i}$,

²A ranker model has to compute layers $L + 1$ onward online.

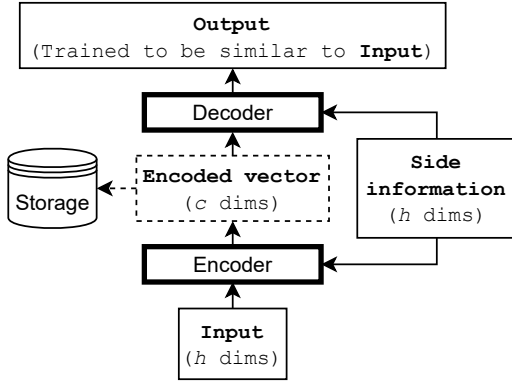


Figure 3: AutoEncoder with Side Information (AESI) architecture. For our usage, the input is the contextual token embedding (the L -th layer’s output), and the side information is the static token embedding (the output of BERT’s initial embedding layer). The resulting c -dimensional encoded vector can be thought of as the distilled context of the input token.

$W_1^d \in \mathbb{R}^{i \times (c+h)}$, $W_2^d \in \mathbb{R}^{h \times i}$ are trainable parameters. h is the dimension of token embeddings (e.g., 384), i is the intermediate autoencoder size, and c is the dimension of the projected (encoded) vector. $\text{gelu}(\cdot)$ is a non-linear activation function [19]. Additional autoencoder variations are explored in § 5.2.

3.2 Quantization

Storing the compressed contextual representations in a naive way consumes 32 bits (float32) per coordinate per token, which is still costly. To further reduce storage overhead, we propose to apply a quantization technique, which uses a predetermined B bits per coordinate. We rely on a recently proposed quantization approach, DRIVE [40], which we describe next and summarize in Algorithm 1. Later in this subsection, we show how we apply DRIVE to our AESI-encoded documents.

Before going into the details of the quantization method, we first require the following definitions:

DEFINITION 1 ([22]). A normalized Walsh-Hadamard matrix, $H_{2^k} \in \{+1, -1\}^{2^k \times 2^k}$, is recursively defined as

$$H_1 = 1; \quad H_{2^k} = \frac{1}{\sqrt{2}} \begin{pmatrix} H_{2^{k-1}} & H_{2^{k-1}} \\ H_{2^{k-1}} & -H_{2^{k-1}} \end{pmatrix}.$$

DEFINITION 2 ([1]). A randomized Hadamard transform, \mathcal{H} , of a vector, $x \in \mathbb{R}^{2^k}$, is defined as $\mathcal{H}(x) := H_{2^k} D x$, where H_{2^k} is a normalized Walsh-Hadamard matrix, and D is a diagonal matrix whose diagonal entries are i.i.d. Rademacher random variables (i.e., taken uniformly from $\{+1, -1\}$). While \mathcal{H} is randomized and thus defines a distribution, when D is known, we abuse the notation and define the inverse Hadamard transform as $\mathcal{H}^{-1}(x) := (H_{2^k} D)^{-1} x = D H_{2^k} x$.

The quantization operates as follows. Given a vector, denoted $x \in \mathbb{R}^d$, we first *precondition* it using a randomized Hadamard transform, \mathcal{H} , and normalize by multiplying by $\sqrt{d}/\|x\|_2$. There are

Algorithm 1 B -bits Vector Quantization (DRIVE) [40]

\mathcal{H} - A randomized Hadamard transform

\mathfrak{C} - K -Means centroids over the normal distribution, where $K = 2^B$

Quantize($x \in \mathbb{R}^d$):

$$y := \frac{\sqrt{d}}{\|x\|_2} \mathcal{H}(x)$$

Compute $X_i = \arg \min_k |y_i - \mathfrak{C}_k|$; $X \in \{0, \dots, 2^B - 1\}^d$

return $X, \|x\|_2$

Dequantize($X, \|x\|_2$):

Compute $\hat{y}_i = \mathfrak{C}_{X_i}$; $\hat{y} \in \{\mathfrak{C}_0, \dots, \mathfrak{C}_{2^B-1}\}^d$

return $\hat{x} = \mathcal{H}^{-1} \left(\frac{\|x\|_2}{\sqrt{d}} \hat{y} \right)$

several desired outcomes of this transform³. First, the dynamic range of the values is reduced (measured, for instance, by the ratio of the ℓ_∞ and the ℓ_2 norms). Loosely speaking, we can think of the transform as spreading the vector’s information evenly among its coordinates. Second, regardless of the distribution of the input vector, each coordinate of the transformed vector will have a distribution that is close to the standard Gaussian distribution (as an outcome of the central limit theorem). After the transform, we perform scalar quantization that is optimized for the $\mathcal{N}(0, 1)$ distribution, using K -means (also known as Max-Lloyd in the quantization literature [14]), with $K = 2^B$. The vector X of cluster assignments together with the original vector’s ℓ_2 norm can now be stored as the compressed representation of the original vector.

To retrieve an estimate of the original vector, we perform the same steps in reverse. We replace the vector of cluster assignments X with a vector \hat{y} containing each assigned cluster’s centroid, denormalize, and then apply the inverse randomized Hadamard transform, \mathcal{H}^{-1} . To avoid encoding D directly, we recreate it using *shared randomness* [31] (e.g., a shared pseudorandom number generator seeded from a hash of the vector’s text). Different variations of the quantization scheme are discussed in § 5.3.

Block-wise Quantization. The AESI encoder reduces the dimension of the contextual embeddings from hundreds (e.g., 384) to a much smaller number (e.g., 12). On the other hand, the randomized Hadamard transform’s preconditioning effect works best in higher dimensions [1]. In order to resolve this conflict, we first concatenate the reduced-dimension vectors of all the tokens from a single document. We then apply the Hadamard transform with a larger block size (e.g., 128) on the concatenated vector, block-by-block (padding the last block with zeros when necessary). When evaluating the compression efficiency, we consider the overhead incurred from (a) the need to store the vectors’ ℓ_2 norms and (b) the padding of the final Hadamard block in a concatenated vector. Balancing these factors should be done per use case.

4 EXPERIMENTAL SETTINGS

In this section, we describe the tasks and datasets used to evaluate the competing approaches, which are evaluated in terms of their quality to rank high relevant text passages for a given query. Next,

³We also note that the transform has the advantage of having a vectorized, in-place, $O(d \log d)$ -time implementation [11].

we describe the baseline and the different configurations of SDR with emphasis on how we measure the compression ratio.

4.1 Evaluation Metrics

We consider two groups of evaluation metrics that capture different aspects of the resulting embeddings, namely:

Ranking: To measure the quality of the reconstructed token embeddings from their compressed vectors c , we consider the two official evaluation metrics in MSMARCO [32]: MRR@10 and nDCG@10 (further discussed below).

Compression: We measure *Compression Ratio* as amount of storage required to store the token embeddings when compared to the distilled baseline. E.g., $CR = 10$ implies storage size that is one tenth of the baseline vectors.

4.2 Tasks and Datasets

To evaluate the effectiveness of our approach SDR and the competing baseline, we use the passage reranking task of MSMARCO [32]. In this task, we are given a query and a list of 1000 passages (retrieved via BM25), and the task is to rerank the passages according to their relevance to the query. We consider two query sets:

MSMARCO-DEV We consider the development set for MSMARCO passage reranking task, which consists of 6980 queries. On average, each query has a single relevant passage, and other passages are not annotated. The performance of models is measured using the mean reciprocal rank, MRR@10, metric.

TREC 2019 DL Track Here we consider the test queries from TREC 2019 DL Track passage reranking dataset. Unlike the above, there are many passages annotated for each query, and there are graded relevance labels (instead of binary labels). This allows us to use the more informative nDCG@10 metric. Due to the excessive annotation overhead, this dataset consists of just 200 queries, so results are more noisier compared to MSMARCO-DEV.

4.3 Baseline – BERT_{SPLIT}

Our algorithm is based on the late-interaction architecture [4, 5, 12, 29, 33] depicted in Figure 2. We created a model based on this architecture, which we name BERT_{SPLIT}, consisting of 10 layers that are computed independently for the query and the document with an additional two late-interaction layers that are executed jointly. We initialized the model from pre-trained weights⁴ and fine-tuned it using knowledge distillation from an ensemble of BERT-Large, BERT-Base, and ALBERT-Large [21] on the MSMARCO small training dataset, which consists of almost 40M tuples of query, a relevant document, and an irrelevant document.⁵

4.4 SDR Configuration and Training

We denote the SDR variants as “AESI- $\{c\}$ - $\{B\}$ b” where $\{c\}$ is replaced with the width of the encoded vector and $\{B\}$ is replaced with the number of bits in the quantization scheme. When discussing AESI with no quantization, we simply write “AESI- $\{c\}$ ”.

Training. SDR requires a pre-training of its autoencoder to minimize its reconstruction error. We train the autoencoder on a random

⁴<https://huggingface.co/cross-encoder/ms-marco-MiniLM-L-12-v2>

⁵The checkpoint will be released with the published paper.

Quant. bits (B)	AESI dim. (c)	Comp. ratio (CR)	MSMARCO-DEV MRR@10	TREC19-DL nDCG@10
32 (float)	16	24	0.3759 (-0.0009)	0.772 (-0.002)
	12	32	0.3725 (-0.0043)*	0.784 (+0.01)
	8	48	0.3711 (-0.0057)*	0.781 (+0.007)
	4	96	0.3660 (-0.0108)*	0.775 (+0.001)
6	16	121	0.3753 (-0.0015)	0.772 (-0.002)
	12	159	0.3728 (-0.004)*	0.780 (+0.006)
	8	231	0.3689 (-0.0079)*	0.775 (+0.001)
	4	423	0.3624 (-0.0144)*	0.766 (-0.008)
5	16	145	0.3735 (-0.0033)*	0.772 (-0.002)
	12	190	0.3714 (-0.0054)*	0.778 (+0.004)
	8	277	0.3649 (-0.0119)*	0.770 (-0.004)
	4	506	0.3540 (-0.0228)*	0.767 (-0.007)
4	16	181	0.3665 (-0.0103)*	0.766 (-0.008)
	12	236	0.3639 (-0.0129)*	0.764 (-0.01)
	8	344	0.3544 (-0.0224)*	0.765 (-0.009)
	4	629	0.3408 (-0.036)*	0.752 (-0.022)*
BERT _{SPLIT} (Baseline)		1	0.3768	0.774

Table 1: SDR performance in various configurations: MRR@10 and nDCG@10 are measured over MSMARCO, as described in § 4.2. The absolute difference w.r.t. the BERT_{SPLIT} baseline is shown in parentheses. We measured statistical significance using relative paired t-test⁶ and denote with * cases with $p < 0.05$. Note that AESI-16-6b shows no significant drop in ranking quality. The compression ratios indicate the reduction in storage size, including padding and normalization overheads.

subset of 500k documents from the total of 8.8M documents present in MSMARCO collection to reduce training time.

Quantization overhead. We incorporate the quantization overhead into the computation of the *compression ratios* as follows: (a) we assume that the additional DRIVE scalar per block (the ℓ_2 -norm) is a float32 and get a space overhead of $32/((\text{block-size}) \cdot B)$ where B is the number of bits in the quantization scheme; and (b) we consider the overhead caused by padding, which depends on the length distribution of documents in the dataset. For the sake of simplicity, we fixed the block size at 128 and measured the padding overhead using a random sample of 100k documents from the MSMARCO-DEV dataset. This measured padding overhead is 20.1%, 9.7%, 6.7%, and 4.5%, for AESI 4, 8, 12, and 16, respectively. In § 5.3, we discuss possible means to reduce this overhead.

5 EVALUATION

In this section, we present the main results on compression ratios and quality tradeoff of the SDR scheme (§ 5.1). Later, we examine how the proposed autoencoder (§ 5.2) and quantization (§ 5.3) compare to other baselines. Finally, in § 5.4, we provide insights and discuss the information captured by our AESI-encoded vectors.

5.1 Main results

Table 1 shows the results on both query sets for SDR and its compression ratio against storing contextual token embeddings uncompressed. In terms of compression ratio, it can be seen that AESI

allows us to massively reduce storage requirements both with and without quantization.

SDR without Quantization: AESI-16 reduces storage requirements by 24x with an insignificant performance drop in $MRR@10$ and $nDCG@10$ compared to the baseline. Higher compression rates can be achieved by further reducing the *context vector*'s dimensions ($c \in \{4, 8, 12\}$) at the cost of having a small but statistically significant lower performance than the baseline. Depending on the use case, such tradeoffs are highly desirable, allowing for extreme compression rates that minimize the costs of deploying Q&A systems. For instance, AESI-12 achieves a 32x compression rate, and although the performance drop is statistically significant, the absolute difference is just 0.0043 for $MRR@10$ (with a tiny increase for $nDCG@10$). In some situations, a better compression rate would justify this slight reduction in performance. Lastly, when using only 4 dimensions for the context vector, we obtain nearly 100x compression rate, fitting the entire MSMARCO collection in less than 11GB of memory.

SDR with Quantization: Highly efficient compression rates and reranking performance is achieved when using quantization techniques. For instance, AESI-16-6b reaches a compression rate of 121x, including padding and normalization overheads, while at the same time showing no significant ranking performance drop. Using AESI-16-6b, a document's embedding can be stored with only 947 bytes, which, as shown in Table 2 in Appendix A, does not add a significant network latency cost in fetching such vectors. The entire MSMARCO collection can be stored within 8.6GB. There are several advantages of fitting the entire collection's representation into the main memory of the hosting machine, allowing for fast access, further fine-tuning, etc. If further compression rates are required, AESI-8-5b uses just 5 bytes per token, reaching a compression rate of 277x and 487 bytes per document on average. At this level of compression, the entire MSMARCO corpus fits in 3.8GB. The $MRR@10$ drop is noticeable (0.0119) but still quite low. Finally, for TREC19-DL, the impact of compressing token embeddings is less evident. Only in the most extreme cases such as AESI-4-4b we see a significant drop in $nDCG@10$ performance. These results demonstrate that the performance drop is very small, showing the effectiveness of our method.

5.2 Autoencoder Evaluation

To better understand the impact of the autoencoder, we present $MRR@10$ results as a function of autoencoder dimensions (i.e., number of floats stored per token) and with the different autoencoder configurations. In addition to the 2-layer AESI architecture we described in § 3.1 (**AESI-2L**), we consider the following variations:

AutoEncoder with 2 Layers (AE-2L). Standard 2-layer autoencoder with gelu activation. This is the same as AESI, only without the side information.

AutoEncoder with 1 Layer (AE-1L). Standard autoencoder with a single dense layer in the encoder and decoder.

AESI with 1 Layer (AESI-1L). AESI with a single dense encoder and decoder layer with side information.

⁶A relative t-test compares systems on the same queries, making it easier to distinguish subtle differences. An independent t-test corresponds to an external observer that only sees results on one system at a time. According to the latter, most of the cases are indistinguishable, except for AESI-{4, 8}-4b and AESI-4-5b.

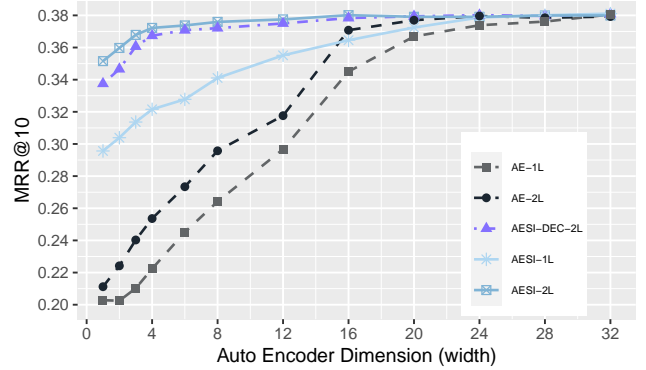


Figure 4: $MRR@10$ was measured on the MSMARCO-DEV-25 dataset as a function of autoencoder dimensions. The results are shown for standard autoencoders (AE) and our approach (AESI), with single or two-layer encoder and decoder networks. The x-axis shows the dimension of the encoded vector c .

DECoder-only AESI (AESI-DEC-2L). Similar to AESI, however the encoder has no access to the side information. Recall that the static token embeddings are required by the decoder to help reconstructing the original vector. This variant checks if the static token embeddings help in the encoding part

To reduce measurement overhead, we ran the experiment over the top 25 $BERT_{SPLIT}$ passages for each query, denoted MSMARCO-DEV-25, which has a negligible impact on the results. Figure 4 shows the results for the different autoencoder configurations. Providing the side information to the autoencoder proves to be very effective in reducing storage costs, especially when the encoded vector size is small. A 2-layer encoder/decoder model, as expected, is more effective than a single-layer model. The gap is especially large when using side information, showing that the interaction between the encoded vector and the static token embeddings is highly nonlinear. Finally, we note that it is possible to provide static token embeddings only to the decoder, but providing it also to the encoder slightly increases the overall $MRR@10$ score.

5.3 Quantization Evaluation

To study the impact of quantization, we fix AESI-16 as our baseline and measure how different quantization strategies and number of bits affect the $MRR@10$ score. Note that we do not measure quantization over the baseline $BERT_{SPLIT}$ since it can only achieve a compression ratio of up to 32x per coordinate (using 1 bit per coordinate). In addition to **DRIVE** (§ 3.2, Algorithm 1), we consider the following quantization strategies:

Deterministic Rounding (DR) [14]. Maps the input coordinates into the $[0, 2^B - 1]$ range using min-max normalization and rounds to the nearest integer.

Stochastic Rounding (SR) [3, 7]. Normalizes as before using min-max normalization, and additionally adds a uniform *dither* noise in $(-0.5, 0.5)$ and then rounds to the nearest integer. This provides an unbiased estimate of each coordinate.

Subtractive Dithering (SD) [15, 36]. Same as SR, only now before denormalization, instead of just using the values in $\{0, \dots, 2^B - 1\}$, we first subtract the original dither noise, which we assume can be regenerated using shared randomness. This is an unbiased estimator with reduced variance.

Hadamard Variants (H-DR, H-SR, and H-SD). These variants correspond to the previous methods; only they are preceded by a randomized Hadamard transform.

DRIVE with Bias Correction (DRIVE-BC) [40, Appendix C.3]. This variant of DRIVE optimizes for lower bias over the mean squared error (MSE) by multiplying the dequantization result in Algorithm 1 by a bias correction scalar: $\|x\|_2^2 / \|\hat{g}\|_2^2$.

Figure 5 shows the results for the different quantization methods. First, we observe that the Hadamard variants perform better than their non-Hadamard counterparts. Second, we see that DRIVE performs better than all other schemes. The differences are more pronounced in the low-bit regime, where the choice of quantization scheme has a drastic impact on quality. We also note that unlike in other use cases, such as distributed mean estimation, bias correction is inappropriate here and should not be performed at the cost of increased mean squared error (MSE). This conclusion follows by observing that DRIVE and the deterministic rounding methods (DR, H-DR) are respectively better than DRIVE-BC and the stochastic rounding methods (SR, H-SR). We add that the subtractive dithering methods (SD, H-SD), expectedly, work the same or better than their deterministic counterparts since they produce a similar MSE while also being unbiased.

The current quantization scheme requires padding to full 128 blocks. For 4-8 AESI size, the padding overhead may reach 10% – 20% percent. In addition, we send a normalization value per 128-block, which we currently send as a float32 value, adding 4% – 5% additional overhead. Padding can be reduced by treating the last 128-block separately, e.g., applying a method that does not require Hadamard transform. Normalization overhead can be reduced, e.g., by sending normalization factors as float16 instead of full float32. However, such solutions complicate the implementation while providing limited storage benefits, hence, they were not explored in the context of this paper.

Beyond Scalar Quantization. Scalar quantization using a fixed number of bits is a suboptimal technique in general since it does not allocate fewer bits for more frequent cases. Entropy coding [14] can do better in this aspect. However, for the 6-bits case, the measured entropy was just 5.71 bits, so the potential improvement from variable-length coding does not seem to justify the efforts (even before accounting for the overhead incurred by Huffman coding or arithmetic coding). Another direction is to use vector quantization or entropy-constrained vector quantization. To estimate an upper bound on the benefits of such techniques, we use the rate-distortion theory (from the information theory field), which studies the optimal tradeoffs between distortion and compression rate [8]. For a Gaussian source, which is a reasonable approximation of the output of Hadamard transform, it is known that the optimal (lossy) compression rate is given by $\frac{1}{2} \log_2(\frac{1}{MSE})$. Compared to the 6-bits case, the optimal rate is 5.35 bits, indicating an upper bound of 11%; results for different bit rates are similar. Therefore, we conclude that the limited gains do not seem to justify the added system complexity.

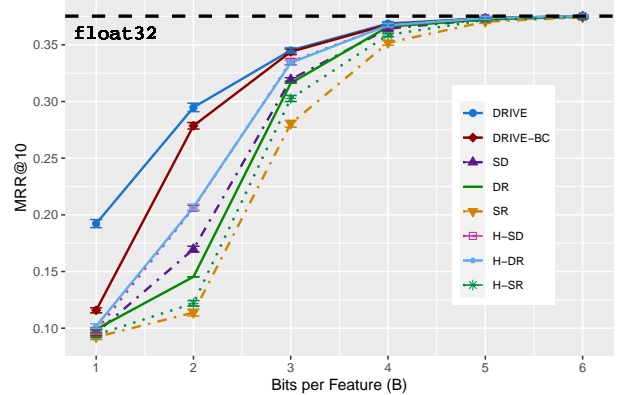


Figure 5: MRR@10 for different quantization methods. Each run quantizes and dequantizes AESI-16 encoded documents over the MSMARCO-DEV-25 dataset. For each randomized quantization method and number of bits, we take the average of 10 runs (the error bars show the standard deviation).

5.4 Intrinsic Evaluation of AESI-Encoded Vectors

In the previous sections, we showed the effectiveness in ranking and utility in compression rates of AESI over AE architectures. However, such evaluations do not capture the encoded information at the token-level. In this intrinsic evaluation we try to discern when and why adding the static embedding as side information contributes to better capturing the token meaning.

We study the effectiveness of different autoencoder configurations in reconstructing back the original token vector, as measured through the MSE between the original vector and the reconstructed vector:

$$MSE(v, D(E(v, u), u)),$$

where v is a contextualized vector (BERT_{SPLIT} output at layer 10), u is the static embedding, and the encoder $E(v, u)$ and the decoder $D(e, u)$ are as defined in § 3.1. High MSE scores indicate the inability of the autoencoder to encode the original vector’s information.

Document Frequency: One way to assess the importance of a document w.r.t. a query is through the inverse document frequency of query tokens, typically measured through TF-IDF or BM25 schemes [37]. In principle, the more infrequent a query token is in a document collection, the higher the ranking of a document containing that token will be. Tokens with (very) high frequencies are typically stop words or punctuation symbols, which have lower importance when determining the query-document relevance.

Based on this premise, we study how MSE varies across token frequency. We selected a random sample of 256k documents from MSMARCO, tokenized them, and run them through BERT_{SPLIT} to get 20M contextualized token representations. Then, for each token we measured their document frequency as $DF(t) = \log_{10}(|\{d \in D : t \in d\}|/|D|)$ (where D is our document collection), and in Figure 6 we plot the average MSE against the rounded DF scores. From this experiment, we make the following observations.

First, on all encoded width configurations, our approach, AESI, consistently achieves lower MSE compared to the AE architecture (for all DF values). Lower MSE correlates to a better ranking quality, as shown in § 5.2. Furthermore, for tokens with low DF, adding the

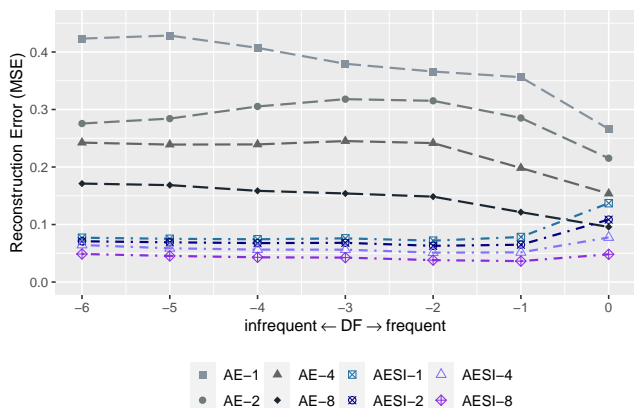


Figure 6: Reconstruction Error vs. DF for the different AE and AESI configurations. AESI shows robust performance in recovering back the token’s representation with a MSE score (y-axis), which is constant for documents with varying DF scores. It is interesting to note that for frequent tokens (i.e., tokens that are function words, hence play a marginal role in retrieval), the error rate is higher when compared to the rest of the tokens.

static side information during the training of AESI for compression provides a huge advantage, which shrinks when the token is present in many documents in the collection.

Second, on the end spectrum of high-frequency tokens, we note a downwards trend for AE and an upwards trend for AESI, especially for $DF \in [-1, 0]$. The MSE decrease for AE is expected since the training data contains more frequent tokens. The increase for AESI can be explained given that in this frequency range, we deal with tokens that are function words (e.g., ‘the’) whose role is more in tying up content within a sentence and has less standalone meaning. In this case, static embeddings cannot capture context, which reduces the contribution provided by the side information.

6 CONCLUSION

In this paper, we proposed a system called SDR to solve the storage cost and latency overhead of existing late-interaction models. The SDR scheme uses a novel autoencoder architecture that uses static token embeddings as side information to improve encoding quality. In addition, we explored different quantization techniques and showed that the recently proposed DRIVE (without bias correction) performs well in our use case and presented extensive experimentation. Overall, the SDR scheme reduces pre-computed document representation size by 4x–11.6x compared to a baseline that uses existing approaches.

In future work, we plan to continue investigating means to reduce pre-computed document representation size. We believe that additional analysis of BERT’s vector and their interaction with the context would be fundamental in such an advancement.

A APPENDIX: LATENCY OVERHEAD OF FETCHING LARGE VECTORS

Existing work, such as PreTTR [29], argue for (some) compression to reduce storage cost. In this appendix, we argue that compression

payload size	200 documents	1000 documents
2	6.4±0.8	21.9±1.5
512	7.0±1.1	24.9±0.5
1K	7.7±0.6	30.6±0.5
2K	9.7±0.5	42.9±6.6
4K	13.2±0.6	55.1±1.4
8K	21.6±0.7	99.7±2.8
16K	38.4±1.1	191.0±5.2
32K	76.9±1.9	391.8±11.

Table 2: Elasticsearch retrieval latency (in milliseconds, ± denotes standard deviation) as a function of payload size and number of fetched documents.

should also be done to reduce the fetching latency of document representation, which, without sufficient compression, can offset any benefits from reducing computation costs.

Standard ad-hoc retrieval is composed of a retrieval service, such as Elasticsearch⁷, which stores the entire corpus, and given an online user, request returns a set of K documents, where K is typically between 100 and 1000. Normally, the retrieval service is the only location where the entire corpus is stored, so it is a natural location for storing pre-computed document embeddings. Therefore, it is important to understand how retrieval latency changes when the size of pre-computed embeddings varies.

Towards answering this question, we measured how Elasticsearch retrieval latency varies with different payload sizes. The full evaluation setup is deferred to the supplementary material for lack of space. The results appear in Table 2. We note that 1KB roughly corresponds to AESI-16-6b, while 512 bytes roughly corresponds to AESI-8-6b. At this range, the latency increase is minimal. However, the payload size for the baseline system is at least 4x larger, leading to a notable latency increase. The original PreTTR work [29] considered up to 12x size reduction, leading to 32K document embedding size. As can be seen in the table, this results in a prohibitively large latency overhead.

REFERENCES

- [1] Nir Ailon and Bernard Chazelle. 2006. Approximate Nearest Neighbors and the Fast Johnson-Lindenstrauss Transform. In *Proceedings of the Thirty-Eighth Annual ACM Symposium on Theory of Computing* (Seattle, WA, USA) (STOC ’06). Association for Computing Machinery, New York, NY, USA, 557–563. <https://doi.org/10.1145/1132516.1132597>
- [2] Dan Alistarh, Demjan Grubic, Jerry Li, Ryota Tomioka, and Milan Vojnovic. 2017. QSGD: Communication-Efficient Sgd via Gradient Quantization and Encoding. *Advances in Neural Information Processing Systems* 30 (2017), 1709–1720.
- [3] RCM Barnes, EH Cooke-Yarborough, and DGA Thomas. 1951. An electronic digital computer using cold cathode counting tubes for storage. *Electronic Engineering* (1951).
- [4] Qingqing Cao, Harsh Trivedi, Aruna Balasubramanian, and Niranjan Balasubramanian. 2020. DeFormer: Decomposing Pre-trained Transformers for Faster Question Answering. In *Proceedings of the 58th Annual Meeting of the Association for Computational Linguistics*. 4487–4497.
- [5] Jiecao Chen, Liu Yang, Karthik Raman, Michael Bendersky, Jung-Jung Yeh, Yun Zhou, Marc Najork, Danyang Cai, and Ehsan Emadzadeh. 2020. DiPair: Fast and Accurate Distillation for Trillion-Scale Text Matching and Pair Modeling. In *Findings of the Association for Computational Linguistics: EMNLP 2020*. 2925–2937.

⁷elasticsearch.com

- [6] Xuanang Chen, Ben He, Kai Hui, Le Sun, and Yingfei Sun. 2021. Simplified TinyBERT: Knowledge Distillation for Document Retrieval. In *European Conference on Information Retrieval*. 241–248.
- [7] Michael P. Connolly, Nicholas J. Higham, and Theo Mary. 2021. Stochastic Rounding and Its Probabilistic Backward Error Analysis. *SIAM Journal on Scientific Computing* 43, 1 (2021), A566–A585. <https://doi.org/10.1137/20M1334796> arXiv:<https://doi.org/10.1137/20M1334796>
- [8] Thomas M. Cover and Joy A. Thomas. 2006. *Elements of Information Theory (Wiley Series in Telecommunications and Signal Processing)*. Wiley-Interscience, USA.
- [9] Jacob Devlin, Ming-Wei Chang, Kenton Lee, and Kristina Toutanova. 2019. BERT: Pre-training of Deep Bidirectional Transformers for Language Understanding. In *Proceedings of the 2019 Conference of the North American Chapter of the Association for Computational Linguistics: Human Language Technologies, Volume 1 (Long and Short Papers)*. Association for Computational Linguistics, Minneapolis, Minnesota, 4171–4186. <https://doi.org/10.18653/v1/N19-1423>
- [10] Mohamed Essam, Tong Boon Tang, Eric Tatt Wei Ho, and Hsin Chen. 2017. Dynamic point stochastic rounding algorithm for limited precision arithmetic in Deep Belief Network training. In *2017 8th International IEEE/EMBS Conference on Neural Engineering (NER)*. 629–632. <https://doi.org/10.1109/NER.2017.8008430>
- [11] Bernard J. Fino and V. Ralph Algazi. 1976. Unified matrix treatment of the fast Walsh-Hadamard transform. *IEEE Trans. Comput.* 25, 11 (1976), 1142–1146.
- [12] Luyu Gao, Zhuyun Dai, and Jamie Callan. 2020. EARL: Speedup Transformer-based Rankers with Pre-computed Representation. *arXiv: Information Retrieval* (2020).
- [13] Luyu Gao, Zhuyun Dai, and Jamie Callan. 2020. Modularized Transformer-based Ranking Framework. In *Proceedings of the 2020 Conference on Empirical Methods in Natural Language Processing (EMNLP)*. 4180–4190.
- [14] A. Gersho and R. M. Gray. 1992. *Vector quantization and signal compression*. Kluwer Academic Publishers.
- [15] R.M. Gray and T.G. Stockham. 1993. Dithered quantizers. *IEEE Transactions on Information Theory* 39, 3 (1993), 805–812. <https://doi.org/10.1109/18.256489>
- [16] Ruiqi Guo, Philip Sun, Erik Lindgren, Quan Geng, David Simcha, Felix Chern, and Sanjiv Kumar. 2020. Accelerating Large-Scale Inference with Anisotropic Vector Quantization. In *International Conference on Machine Learning*. <https://arxiv.org/abs/1908.10396>
- [17] Suyog Gupta, Ankur Agrawal, Kailash Gopalakrishnan, and Pritish Narayanan. 2015. Deep Learning with Limited Numerical Precision. In *Proceedings of the 32nd International Conference on Machine Learning (Proceedings of Machine Learning Research, Vol. 37)*, Francis Bach and David Blei (Eds.). PMLR, Lille, France, 1737–1746. <http://proceedings.mlr.press/v37/gupta15.html>
- [18] Kelvin Guu, Kenton Lee, Zora Tung, Panupong Pasupat, and Mingwei Chang. 2020. Retrieval Augmented Language Model Pre-Training. In *ICML 2020: 37th International Conference on Machine Learning, Vol. 1*. 3929–3938.
- [19] Dan Hendrycks and Kevin Gimpel. 2016. Gaussian Error Linear Units (GELUs). *arXiv preprint arXiv:1606.08415* (2016).
- [20] Sebastian Hofstätter, Sophia Althammer, Michael Schröder, Mete Sertkan, and Allan Hanbury. 2020. Improving Efficient Neural Ranking Models with Cross-Architecture Knowledge Distillation. *arXiv preprint arXiv:2010.02666* (2020).
- [21] Sebastian Hofstätter, Markus Zlabinger, and Allan Hanbury. 2020. Interpretable & Time-Budget-Constrained Contextualization for Re-Ranking. In *ECAI*. 513–520.
- [22] Kathy J Horadam. 2012. *Hadamard Matrices and Their Applications*. Princeton university press.
- [23] Xiaoqi Jiao, Yichun Yin, Lifeng Shang, Xin Jiang, Xiao Chen, Linlin Li, Fang Wang, and Qun Liu. 2020. TinyBERT: Distilling BERT for Natural Language Understanding. In *Findings of the Association for Computational Linguistics: EMNLP 2020*. 4163–4174.
- [24] Jeff Johnson, Matthijs Douze, and Hervé Jégou. 2017. Billion-scale similarity search with GPUs. *IEEE Transactions on Big Data* (2017).
- [25] Vladimir Karpukhin, Barlas Oguz, Sewon Min, Patrick S. H. Lewis, Ledell Wu, Sergey Edunov, Danqi Chen, and Wen tau Yih. 2020. Dense Passage Retrieval for Open-Domain Question Answering. In *Proceedings of the 2020 Conference on Empirical Methods in Natural Language Processing (EMNLP)*. 6769–6781.
- [26] Omar Khattab and Matei Zaharia. 2020. ColBERT: Efficient and Effective Passage Search via Contextualized Late Interaction over BERT. In *Proceedings of the 43rd International ACM SIGIR Conference on Research and Development in Information Retrieval*. 39–48.
- [27] Jakub Konečný and Peter Richtárik. 2018. Randomized Distributed Mean Estimation: Accuracy vs. Communication. *Frontiers in Applied Mathematics and Statistics* 4 (2018), 62.
- [28] Wenhao Lu, Jian Jiao, and Ruofei Zhang. 2020. TwinBERT: Distilling Knowledge to Twin-Structured BERT Models for Efficient Retrieval. *arXiv preprint arXiv:2002.06275* (2020).
- [29] Sean MacAvaney, Franco Maria Nardini, Raffaele Perego, Nicola Tonello, Nazli Goharian, and Ophir Frieder. 2020. Efficient Document Re-Ranking for Transformers by Precomputing Term Representations. In *Proceedings of the 43rd International ACM SIGIR Conference on Research and Development in Information Retrieval*. 49–58.
- [30] Avner May, Jian Zhang, Tri Dao, and Christopher Ré. 2019. *On the Downstream Performance of Compressed Word Embeddings*. Curran Associates Inc., Red Hook, NY, USA.
- [31] Ilan Newman. 1991. Private vs. Common Random Bits in Communication Complexity. *Information processing letters* 39, 2 (1991), 67–71.
- [32] Tri Nguyen, Mir Rosenberg, Xia Song, Jianfeng Gao, Saurabh Tiwary, Rangan Majumder, and Li Deng. 2016. MS MARCO: A Human Generated Machine Reading Comprehension Dataset. In *CoCo@NIPS*.
- [33] Ping Nie, Yuyu Zhang, Xiubo Geng, Arun Ramamurthy, Le Song, and Daxin Jiang. 2020. DC-BERT: Decoupling Question and Document for Efficient Contextual Encoding. In *Proceedings of the 43rd International ACM SIGIR Conference on Research and Development in Information Retrieval*. 1829–1832.
- [34] Rodrigo Nogueira and Kyunghyun Cho. 2019. Passage Re-ranking with BERT. *CoRR* abs/1901.04085 (2019). arXiv:1901.04085 <http://arxiv.org/abs/1901.04085>
- [35] Yingqi Qu, Yuchen Ding, Jing Liu, Kai Liu, Ruiyang Ren, Xin Zhao, Daxiang Dong, Hua Wu, and Haifeng Wang. 2020. RocketQA: An Optimized Training Approach to Dense Passage Retrieval for Open-Domain Question Answering. *arXiv preprint arXiv:2010.08191* (2020).
- [36] L. Roberts. 1962. Picture coding using pseudo-random noise. *IRE Transactions on Information Theory* 8, 2 (1962), 145–154. <https://doi.org/10.1109/TIT.1962.1057702>
- [37] Stephen Robertson and Hugo Zaragoza. 2009. *The probabilistic relevance framework: BM25 and beyond*. Now Publishers Inc.
- [38] Victor Sanh, Lysandre Debut, Julien Chaumond, and Thomas Wolf. 2019. DistilBERT, a distilled version of BERT: smaller, faster, cheaper and lighter. *arXiv preprint arXiv:1910.01108* (2019).
- [39] Ananda Theertha Suresh, X Yu Felix, Sanjiv Kumar, and H Brendan McMahan. 2017. Distributed Mean Estimation With Limited Communication. In *International Conference on Machine Learning*. PMLR, 3329–3337.
- [40] Shay Vargaftik, Ran Ben Basat, Amit Portnoy, Gal Mendelson, Yaniv Ben-Itzhak, and Michael Mitzenmacher. 2021. DRIVE: One-bit Distributed Mean Estimation. arXiv:2105.08339 [cs.LG]
- [41] Naigang Wang, Jungwook Choi, Daniel Brand, Chia-Yu Chen, and Kailash Gopalakrishnan. 2018. Training deep neural networks with 8-bit floating point numbers. In *Proceedings of the 32nd International Conference on Neural Information Processing Systems*. 7686–7695.
- [42] Shuang Wu, Guoqi Li, Feng Chen, and Luping Shi. 2018. Training and Inference with Integers in Deep Neural Networks. In *International Conference on Learning Representations*. <https://openreview.net/forum?id=HJGXzmspb>
- [43] Lee Xiong, Chenyan Xiong, Ye Li, Kwok-Fung Tang, Jialin Liu, Paul N. Bennett, Junaid Ahmed, and Arnold Overwijk. 2021. Approximate Nearest Neighbor Negative Contrastive Learning for Dense Text Retrieval. In *ICLR 2021: The Ninth International Conference on Learning Representations*.
- [44] Andrew Yates, Rodrigo Nogueira, and Jimmy Lin. 2021. Pretrained Transformers for Text Ranking: BERT and Beyond. In *Proceedings of the 2021 Conference of the North American Chapter of the Association for Computational Linguistics: Human Language Technologies: Tutorials*. Association for Computational Linguistics, Online, 1–4. <https://doi.org/10.18653/v1/2021.naacl-tutorials.1>

DETAILS OF THE LATENCY OVERHEAD EVALUATION

First, we set up an Elasticsearch cluster using AWS Elasticsearch service⁸. This service is used by multiple companies and can be consider as reproducing “real” production environment. We used default settings for the cluster and set node type to m5.xlarge.

We then created an Elasticsearch index and populated it with documents. To study the effect of fetching latency, we duplicate each document multiple times, each with a different blob (aka payload) size. Specifically, we repeatedly select a random sample of 10 words, and denote these as a document. For each such document, we consider 8 replications, where for each replica we add a blob field with a string of length X, and added a unique size word “SIZE-X” to the

⁸<https://aws.amazon.com/elasticsearch-service/>

document, where X is selected from the possible sizes {2, 512, 1K, 2K, 4K, 8k, 16K, 32K}.

Once the index was populated, we run some warm-up queries against the index, to ensure the index is in a steady state.

During experimentation, we repeatedly query (and fetch) documents with blob size of X and measure how retrieval time changes with X . Each query is composed of a `should clause`⁹ with 3 randomly selected words, and a `must clause` with the word “SIZE- X ”, which ensures that only documents with blob size X are returned. The number of documents to retrieve is limited to 1000 (as

the default configuration of MSMARCO passage ranking task) or 200. All queries are executed by a single thread to avoid concurrency interference and queuing effects, on an AWS EC2 machine in the same datacenter as the Elasticsearch cluster. Each experiment issues 100 queries and is repeated 30 times, while interleaving different X values to avoid potential biases. We report the average time in milliseconds (ms) and standard deviation in Table 2.

⁹<https://www.elastic.co/guide/en/elasticsearch/reference/current/query-dsl-bool-query.html>